

MATHSM: Medial Axis Transform toward High Speed Machining of Pockets

Gershon Elber* and Elaine Cohen† and Sam Drake‡

December 31, 2003

Abstract

The pocketing operation is a fundamental procedure in NC machining. Typical pocketing schemes compute uniform successive offsets or parallel cuts of the outline of the pocket, resulting in a toolpath with C^1 discontinuities. These discontinuities render the toolpath quite impractical in the context of high speed machining.

This work addresses and fully resolves the need for a C^1 continuous toolpath in high speed machining and offers MATHSM, a C^1 continuous toolpath for arbitrary C^1 continuous pockets. MATHSM generates a C^1 continuous toolpath that consists of primarily circular arcs while maximizing the radii of the generated arcs and, therefore, minimizing the exerted radial acceleration.

Key Words: Voronoi diagrams, Medial Axis Transform, High Speed Machining, Lines and Arcs, Bi-arcs.

1 Introduction and Related Work

Pocketing is one of the most common operations in NC machining applications [2, 3, 5, 9, 10, 11, 12, 15, 18, 19, 21]. For example, forming die-cavities [2] is one such application. It requires machining at different levels of several parallel cutting planes that define various pockets. A closed shape, denoted the *outline* of the pocket, is prescribed in a pocketing operation, possibly with islands, and a toolpath is generated to machine the interior of the shape, cleaning it to a prescribed depth. In many applications the bottom of the pocket is planar, an assumption we make in this paper unless otherwise stated. We consider possible extensions to non-planar bottoms toward the end of this paper.

Two major approaches exist to generate toolpaths for pocketing operations. The first is based on the intersection of the outline of the pocket with parallel and equally spaced planes. By connecting

*Computer Science Department, Technion, Israel E-mail: gershon@cs.technion.ac.il

†Computer Science Department University of Utah, SLC, Utah, USA E-mail: cohen@cs.utah.edu

‡Computer Science Department University of Utah, SLC, Utah, USA E-mail: drake@cs.utah.edu

the parallel adjacent segments that trim the pocket domain into a zig-zag motion, a complete toolpath is constructed [10, 18, 19]. This approach is similar to the scan conversion scheme used in computer graphics to render polygonal domains and fill them with pixels [8]. The different scanline segments are then connected into a C^0 continuous zigzag toolpath.

The second approach offsets the outline(s) of the pocket by equally spaced offset distances, and employs these successive offsets to derive a toolpath [9, 15, 3]. Offsets of a C^1 continuous outline can yield C^1 discontinuities in regions where the radius of curvature of the curve is larger than the offset distance. Hence, in general, this offset-based toolpath is also C^0 continuous.

Both schemes typically work with outlines formed from lines and arcs. Use of lines alone to approximate the outline risks the loss of C^1 continuity in the outline's approximation. Hence, it is desirable to use arcs as well as lines, in the approximating the outline. This makes it possible to achieve C^1 continuity where the radius is larger than the offset distance and, also, since many NC machines support an arc instruction, it reduces the size of the generated G-codes.

One approach to machining pockets with freeform curve outlines is to approximate the freeform shape using arcs [1, 2, 14]. Usually, the error between the freeform spline curve and two successive arcs, or bi-arcs, is approximated simultaneously, achieving the ability to approximate inflection points in the curve. Errors are typically measured in the L^∞ sense, although the L^2 norm has been employed as well [14].

Offset computation directly from the freeform outline curve is also quite common and robust (see [4] for a recent survey), and is desirable for several reasons. The parameterization of the original curve can be preserved, and hence, the association between the original geometry and its offset is maintained. In addition, the resulting offset consisting of spline segments can be more efficiently downloaded to an NC machine that supports spline motion interpolation. Finally, the bi-arcs approximation introduces another phase of approximation that also increases the data sets. The problem, however, of clipping or trimming the self-intersecting freeform curves in the resulting offsets is considered a difficult one. In [5], analytic distance maps are employed to robustly trim both local and global self-intersections in offsets of freeform curves. The direction of robust toolpath generation using direct spline offset computations should, therefore, be further pursued.

Other related works on NC pocket operations have attempted to look at optimization issues. Examples include consideration of successive application of tools with decreasing radii [21], so as to reduce the overall machining time, or alternatively, minimizing the number of retractions in zigzag [18, 19] and offset [3] type toolpaths. The latter has an exponential-expected time complexity due to the ability of reducing the toolpath traversal problem to the Travelling Salesman Problem (TSP).

High speed machining (HSM) is an NC machining procedure that is becoming more and more common [13, 17, 20]. Unfortunately, both the zigzag toolpath and the offsetting toolpath generation approaches introduce multiple C^1 discontinuities into the toolpath, making it unsuitable for high speed machining applications. Recently, several attempts have been made to alleviate these difficulties. One approach employs a spiral motion that starts at the center of the pocket and spirals out until it reaches the outline [13, 17]. The spiral toolpath has an infinite curvature at the limit, if the spiral starts at the center. Furthermore, it is unclear how to initialize the spiraling process as well as bring the tool to its proper cutting depth. While the spiraling scheme can work reasonably well in almost circular pockets, it also becomes arbitrarily inefficient when elongated pockets are considered. Similar difficulties might result when pockets with complex shapes are considered. Other approaches include trochoidal milling [20] where the toolpath is following a trochoidal path. This scheme is used mainly to handle locally C^1 discontinuities in the pocket outline, converting C^1 discontinuities into small loops that connect the adjacent pieces, thereby forming a C^1 continuous toolpath.

In our work, we propose a different scheme to handle the high speed machining of arbitrary C^1 continuous pockets. The generated toolpath consists of arcs of as-large-as-possible radii, or half that much, and possibly, line segments. Further, the constructed toolpath is guaranteed to be C^1 continuous, maximizing the benefits that can be drawn from the high speed machining schemes.

In Section 2, the basic algorithm is considered. In Section 3, several examples are presented, including NC machining tests we have conducted. In Section 4, several possible extensions are discussed and finally, we conclude in Section 5.

2 The Basic MATHSM toolpath Algorithm

Given a freeform closed curve, $C(t)$, possibly with islands, $I_i(t_i)$, we seek the medial axis transform (MAT) of the geometry for reasons to be explained shortly. Robust algorithms to approximate the MAT of freeform curves in the plane have begun to appear [6, 7, 16]. Alternatively, one can employ one of the existing piecewise bi-arc and/or piecewise line-arc approximation methods for freeform curves and use MAT computation for lines and arcs—an approach that nowadays is considered robust. For example, the VRONI [12] package derives the MAT of outlines formed of lines and arcs. In this work, and in all presented examples, the VRONI package was used to derive the MAT by first converting the freeform spline into a bi-arc approximation with prescribed tolerance.

By definition, the MAT fully prescribes the maximal circles one can fit into any location of the pocket to be machined (see Figure 1). Denote such circles as *Maximally Inscribed Circles* (MICs). The MAT

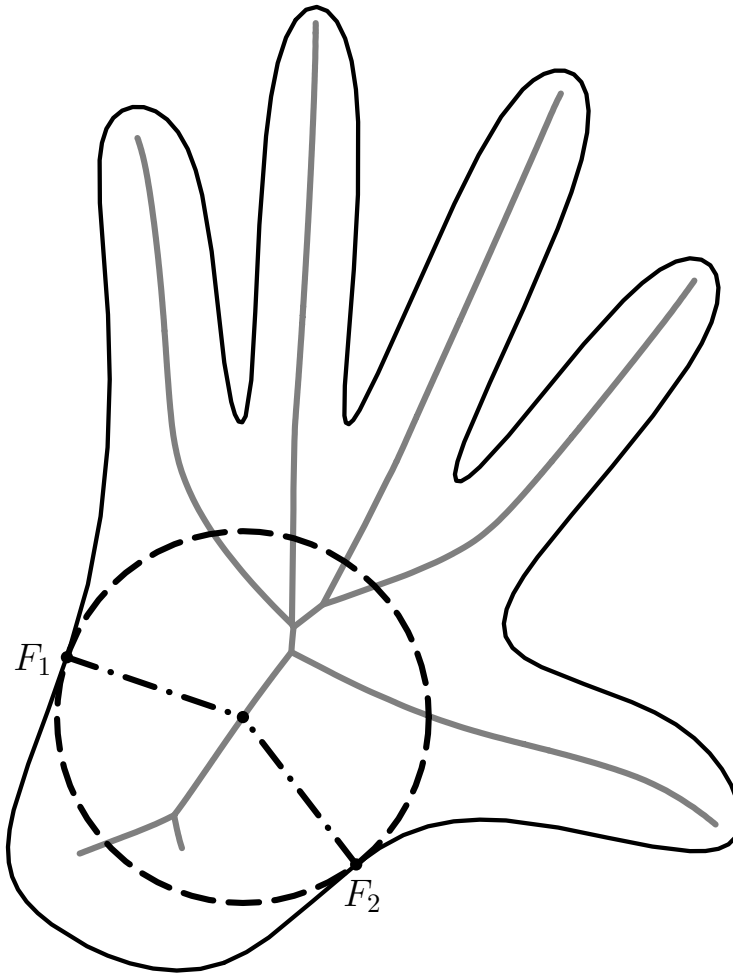


Figure 1: A pocket with an outline in the shape of a human hand is presented. In thick gray lines, the MAT of the outline is presented. Also shown is one Maximally Inscribed Circle (MIC) along with its typically two foot points, F_1 and F_2 . The foot points are provided by the MAT data structure, for all points on the MAT.

provides excellent cues to build a toolpath from successive MICs, following discrete steps along the MAT. Since accelerations should be minimized in high speed machining, by using MICs one is offered the best complete circular motions that are possible at those pocket locations. The MIC is the largest circle that fits any pocket location, and hence the MIC prescribes the motion that minimizes the radial accelerations among all circular motions in that local neighborhood. By connecting successive MICs using bi-tangent lines (see Figure 2), one can construct a full and complete toolpath that will machine the entire pocket.

This short overview of the proposed toolpath generation approach portrays the essence of this work. The toolpath is constructed using successive MICs and small bi-tangent line segments connect the successive

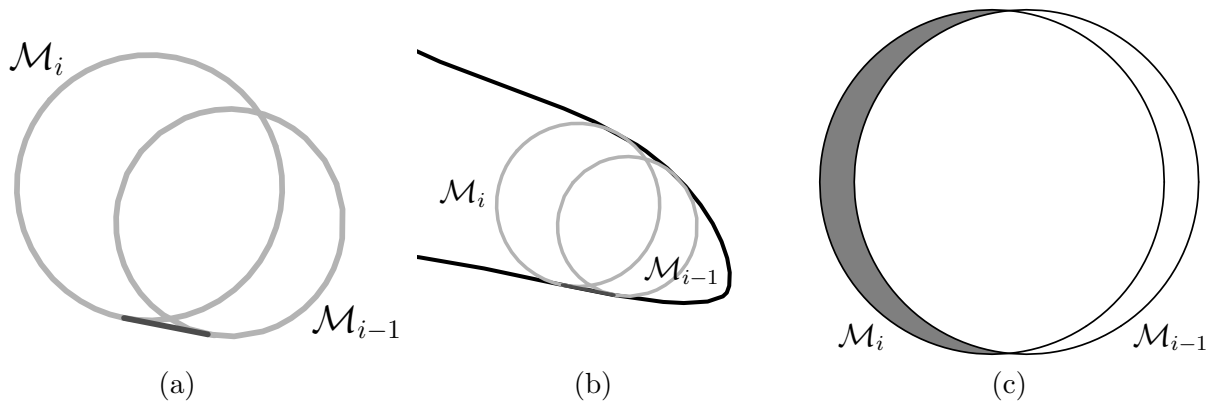


Figure 2: Successive MICs (light gray) are connected using a line segment tangent to both circles (in dark gray), yielding a scheme that achieves a C^1 continuous toolpath. In (a), the two circles are isolated out of the pocket, whereas in (b), they are shown inside the pocket. In (c), the new material that is removed between two successive MICs is shown in gray.

MICs. Because, in practice, successive MICs possess somewhat different radii and are not necessarily centered along a straight line, each MIC could be traversed less than or more than 360 degrees (see Figure 2). Clearly, the spacings of the MICs is closely related to the amount of material removed during the machining process and the quality of the result. Let \mathcal{M}_i be the i th MIC in the toolpath. Then, when executing the motion of \mathcal{M}_i , the tool removes the material in $\mathcal{M}_i - \mathcal{M}_{i-1}$. The shape of the removed material is shown in Figure 2 (c). The amount of material that the tool removes while traversing \mathcal{M}_i changes continuously, gradually increasing and then decreasing, making the load change on the tool continuous. Nonetheless, the geometry of the material removed also means that, in general, we are machining about half the time using this toolpath scheme. When the tool is traversing the MIC's path \mathcal{M}_i , it cuts nothing when it is completely contained in the MIC \mathcal{M}_{i-1} . It can only remove material when in contact with $\mathcal{M}_i - \mathcal{M}_{i-1}$. We will partially address this shortcoming in Section 4. We denote the toolpath generation scheme, shown in Figure 3, as the *central* MATHSM toolpath because the centers of the MICs are placed on the MAT of the outline.

Two circles can have up to four different bi-tangent line segments. Let $\mathcal{C}_i = (c_i^x, c_i^y)$ and r_i be the center point and radius of MIC \mathcal{M}_i , respectively, and consider line $Ax + By + C = 0$. Then, the four bi-tangent line segments between \mathcal{M}_i and \mathcal{M}_{i-1} are the solutions of the following constraints:

$$\begin{aligned} 1 &= A^2 + B^2 \\ \pm r_i &= Ac_i^x + Bc_i^y + C, \end{aligned}$$

$$\pm r_{i-1} = Ac_{i-1}^x + Bc_{i-1}^y + C, \quad (1)$$

having three equations and three unknowns, A , B , and C . The first equation in Constraints (1) ensures that the line representation is unique. The second and third equations guarantee that the distance between the line and the MICs' centers equates with the circles' radii. By solving for A and B , employing Cramer's rule, as a function of C using the last two equations of (1), one gets,

$$A = \frac{\begin{vmatrix} \pm r_i - C & c_i^y \\ \pm r_{i-1} - C & c_{i-1}^y \end{vmatrix}}{\begin{vmatrix} c_i^x & c_i^y \\ c_{i-1}^x & c_{i-1}^y \end{vmatrix}} = mC + n, \quad B = \frac{\begin{vmatrix} c_i^x & \pm r_i - C \\ c_{i-1}^x & \pm r_{i-1} - C \end{vmatrix}}{\begin{vmatrix} c_i^x & c_i^y \\ c_{i-1}^x & c_{i-1}^y \end{vmatrix}} = pC + q, \quad (2)$$

for some $m, n, p, q \in \mathbb{R}$. Substituting A and B into the first constraints of (1), the solution of the quadratic equation is C . Having C , one can resolve A and B using Equation (2), completing the solution.

Two equations in Constraints (1) have a sign (\pm) degree of freedom, suggesting four possibilities overall. Nonetheless, and noting that lines (A, B, C) and $(-A, -B, -C)$ are the same, all that is necessary is to differentiate the case where both centers are on the same side of the line (external bi-tangent) or both centers are on the opposite side of the line (internal bi-tangent). Interested in external bi-tangents only, we need only find the solution of Constraints (1) such that both constraints share the same sign.

Assuming we would rather move in an always-clockwise or always-counter-clockwise direction for all MICs and throughout the toolpath, only the two external bi-tangents are of interest. One can select either one of the two external bi-tangents, corresponding to clockwise or counter-clockwise toolpaths, two options that are shown in Figure 3 (a) and (b), respectively. As can be seen by inspecting Figure 3, convex outline regions are better machined when bi-tangent lines connect the successive MICs along the convex edge. Yet, concave outline regions are better left unconnected (connecting the successive MICs using their other external bi-tangent), else gouging might occur. In Section 4, we will consider a simple extension to this bi-tangent line segment connection approach that will significantly improve the quality of the finished machined outline, for both convex and concave outline regions.

The MAT is a tree when no islands are introduced in the outline, and shares the same genus with the pocket when islands are present. In either case, each leaf of the MAT will amount to one retraction in the toolpath. Since retractions are expensive in high speed machining, we also consider an alternative traversal of the MAT. Instead of placing the tool's center along the MAT, the tool will traverse the path while the MAT is always to its left (or its right), placing the tool's center mid-way from a MAT point to its foot points (recall Figure 1), the support points where the MIC is tangent to the outline. Provided there are no islands in the given pocket, we now cover the entire domain of the pocket in a single loop and no

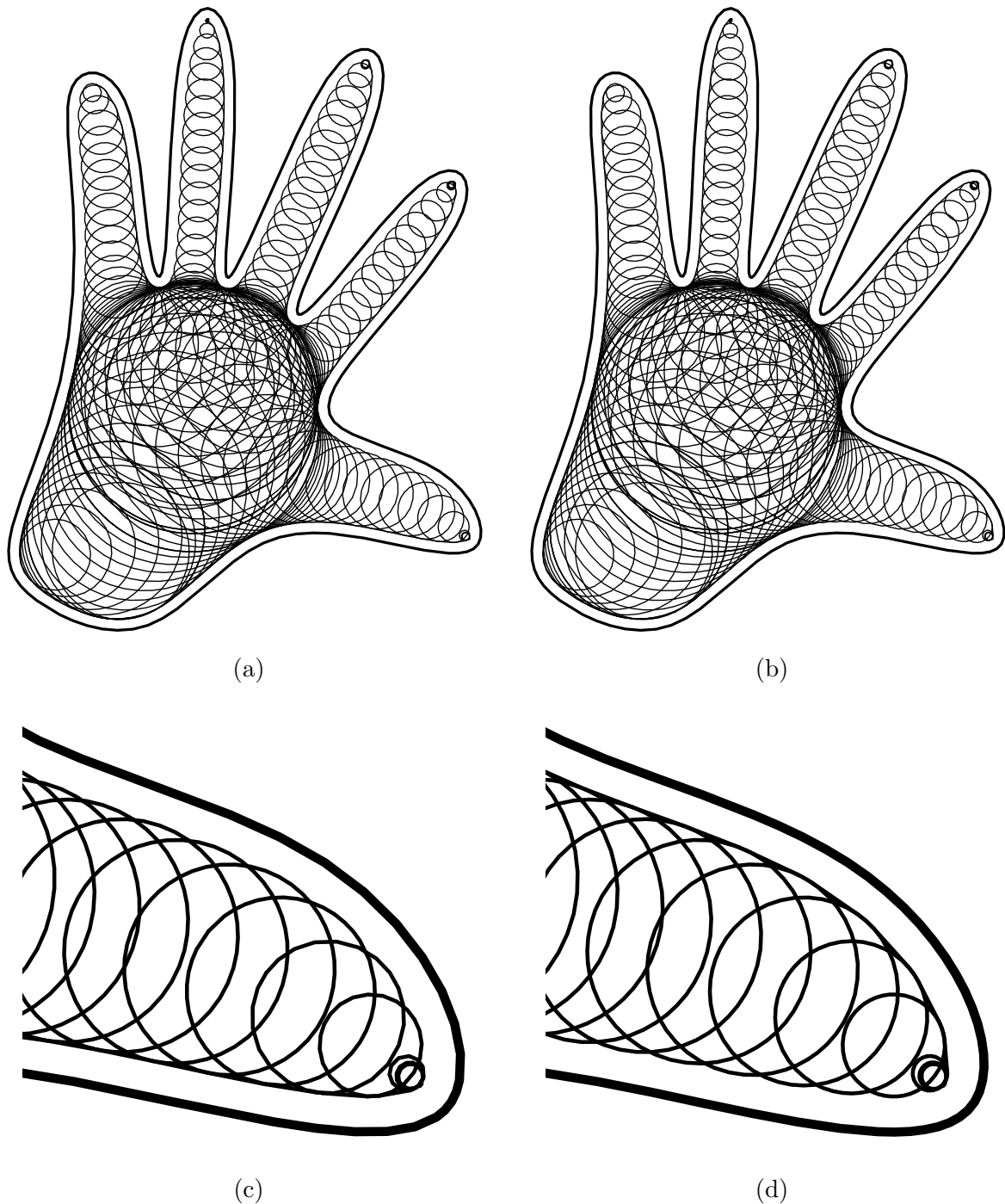


Figure 3: A C^1 continuous *central* toolpath for a flat end tool for a human hand is connected using left line segments, creating a toolpath with CW rotations (a) and using right line segments, creating a toolpath with CCW rotations (b). (c) and (d) show the thumb of (a) and (b), respectively, scaled up.

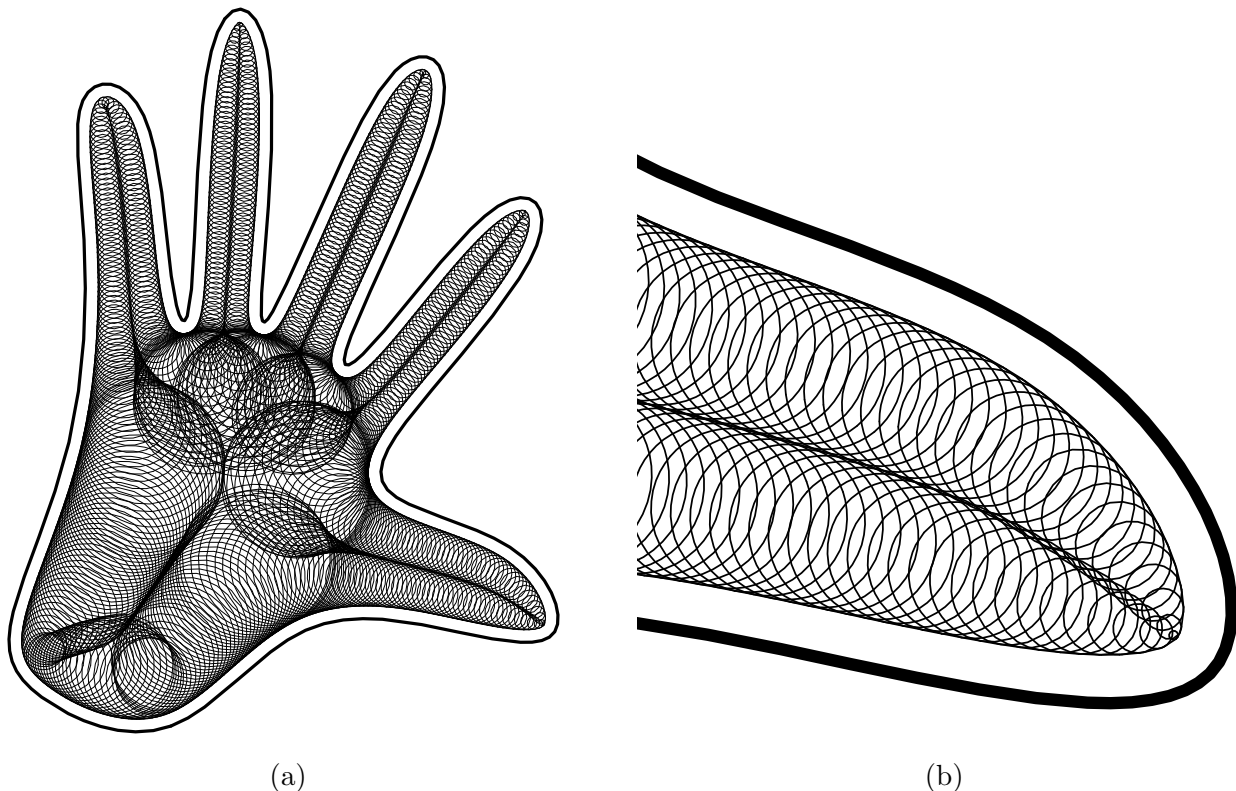


Figure 4: In (a), a modification of the central approach presented in Figure 3 as a C^1 continuous *one-sided* toolpath that virtually removes all necessary retractions at the cost of halving the arcs' radii in the toolpath is presented. (b) presents a scaled up view of the thumb.

intermediate retractions are necessary. Having islands in the pockets and hence loops in the MAT, we will be forced to retract once per loop, a condition one could somewhat relax in many cases, as we will see in Section 4. We denote this toolpath a *one-sided* MATHSM toolpath.

The toolpath will now look at can be seen in Figure 4. The cost of this modified, one-sided approach that eliminates the retractions is obvious. We are now machining with half the optimal radius. Using the one-sided toolpath, the line segments connecting the successive MICs will all be along the outline or will all be in the interior, along the MAT; see Figure 5.

3 Examples of the HSM toolpath algorithm

We have tested the one-sided HSM toolpath, which we foresee as overall somewhat superior to the central scheme, on three different examples. Figure 6 shows the human hand pocket from Figure 4 machined in aluminum. Figure 7 shows a pocket in the shape of the letters 'GE', using the toolpath from Figure 5 machined in aluminum. Finally, Figure 8 shows one half of a mold machined at two levels of a rounded square

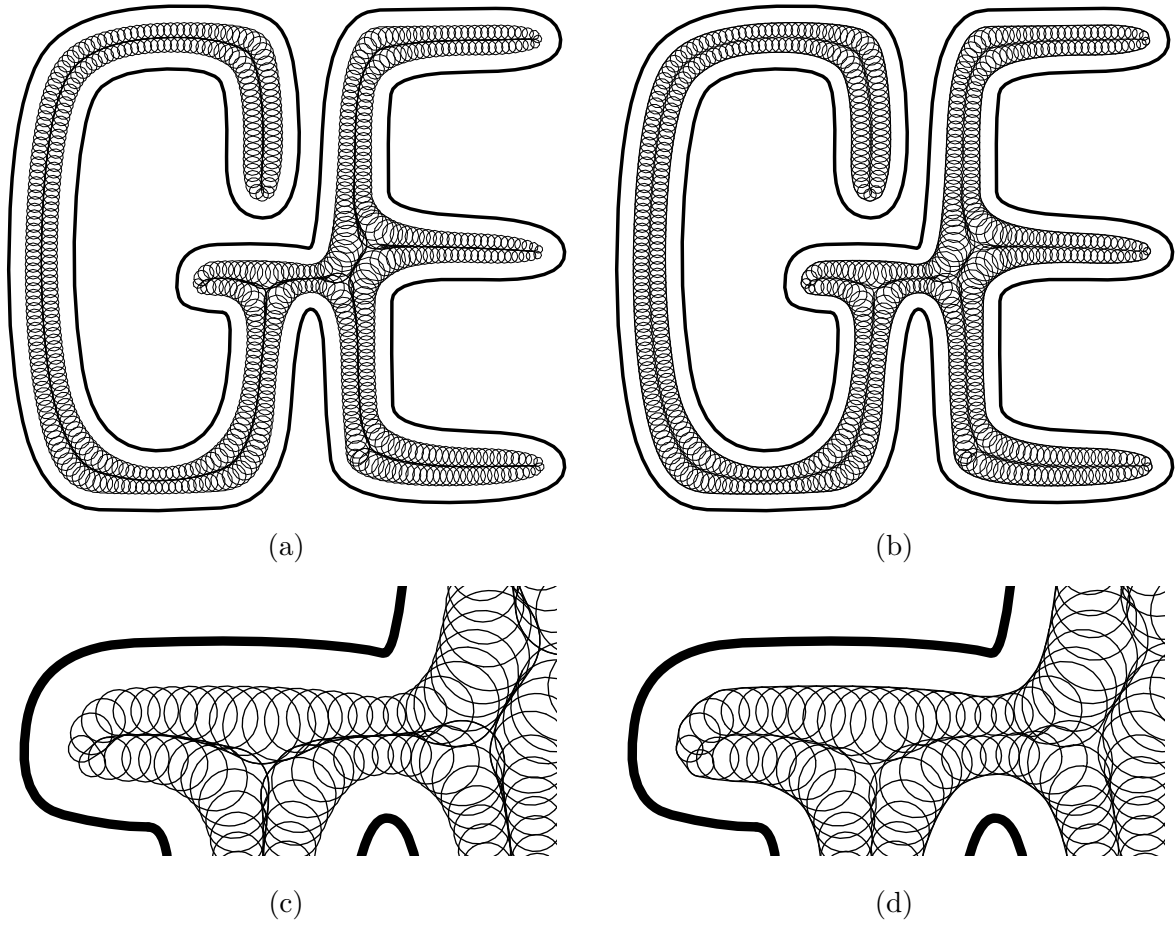


Figure 5: A C^1 continuous central toolpath for the 'GE' letters pocket is connected using inside line segments along the MAT (a) and outside line segments along the outline (b). (c) and (d) show the central regions of (a) and (b) scaled up, respectively.

pocket, and then a four-circular-satellites pocket shape. Figure 8 (a) shows the toolpath of the rounded square pocket and Figure 8 (b) presents the toolpath of the four-circular-satellites pocket. Figure 8 (c) and (d) presents the part machined in aluminum.

As can be seen in all three examples, the proposed scheme performs well in elongated and skinny regions, regions in which traditional pocketing schemes do poorly. The presented approach is not efficient in large rounded pockets such as the large palm region of the hand in Figure 4 (a) or the rounded square of the mold in Figure 8 (a). This lack of efficiency is shown by the significant overlaps of different MICs of unrelated branches of the MAT of the outline.

It is important to initialize the tool, that is, bring the tool to its proper initial depth, while preserving the C^1 continuity of the toolpath and minimizing accelerations. One can select one MIC in the toolpath that is not too small and spiral down along that MIC in a helical motion for several rounds until the proper

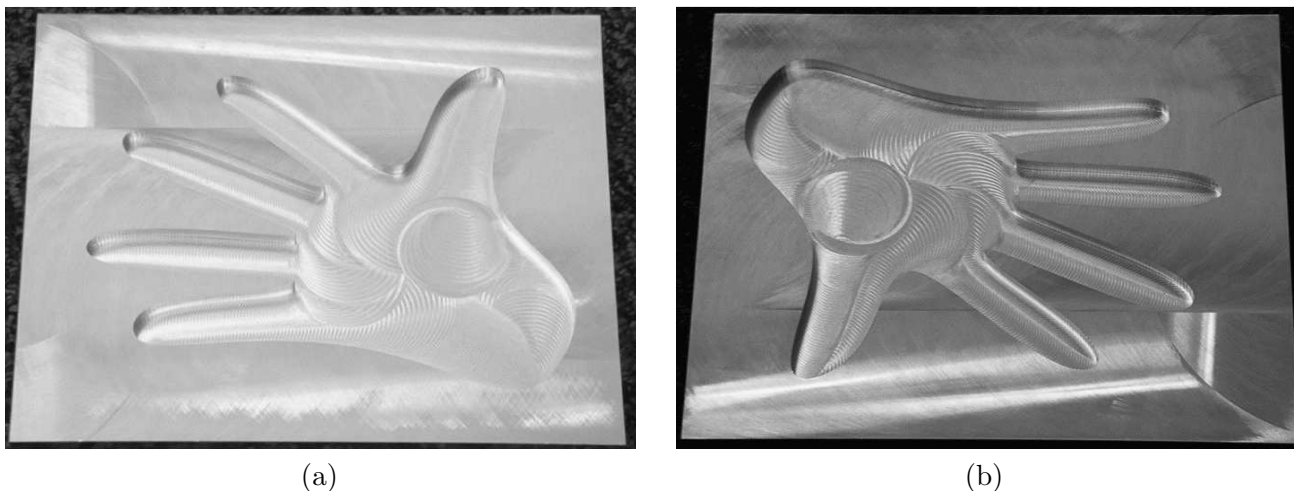


Figure 6: Two views of the hand machined in aluminum are presented. See the toolpath in Figure 4.

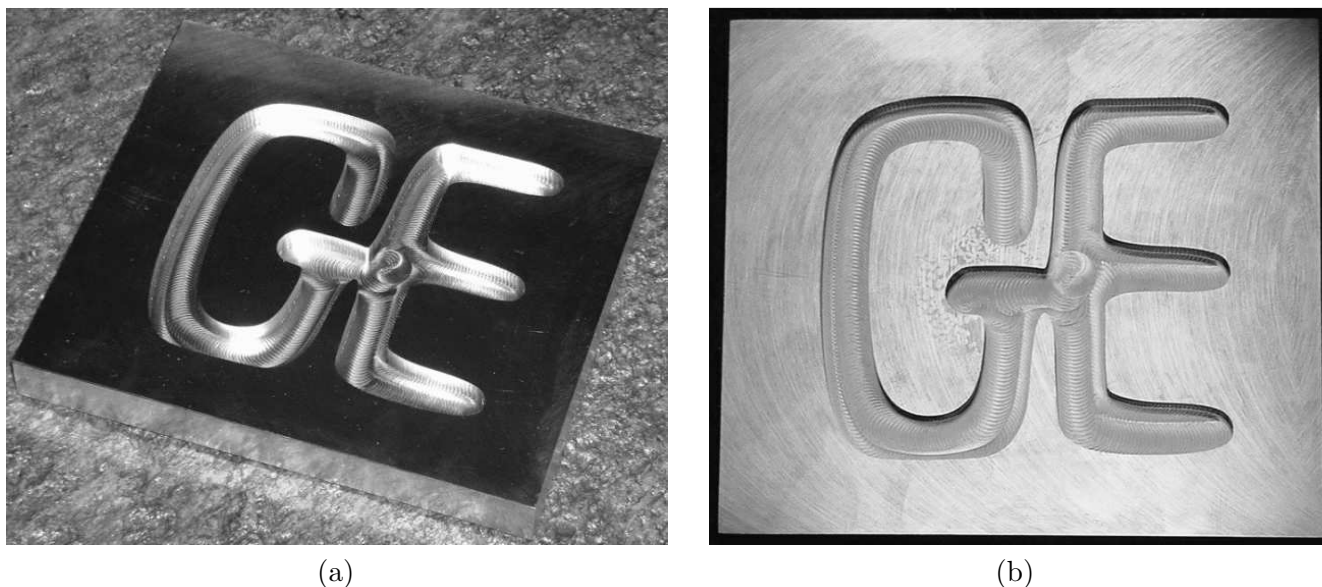


Figure 7: Two views of the 'GE' part machined in aluminum are presented. See the toolpath in Figure 5.

depth is reached. Then, the regular toolpath is used at the current depth, visiting the successive MICs until the entire toolpath is traversed.

4 Extending the MATHSM Toolpath Algorithm

The MATHSM toolpath generation scheme as presented so far attempts to connect successive MICs, with the aid of bi-tangent line segments, to successive circles. However, with a little effort, one can do considerably better. Consider the curved segment of the outline between two successive MICs, \mathcal{M}_i and \mathcal{M}_{i-1} (see Figure 9). One can fit an arc bi-tangent to both \mathcal{M}_i and \mathcal{M}_{i-1} that better approximates the shape of the outline. In Figure 9 (a), a line connects the two successive MICs whereas in Figure 9 (b) a

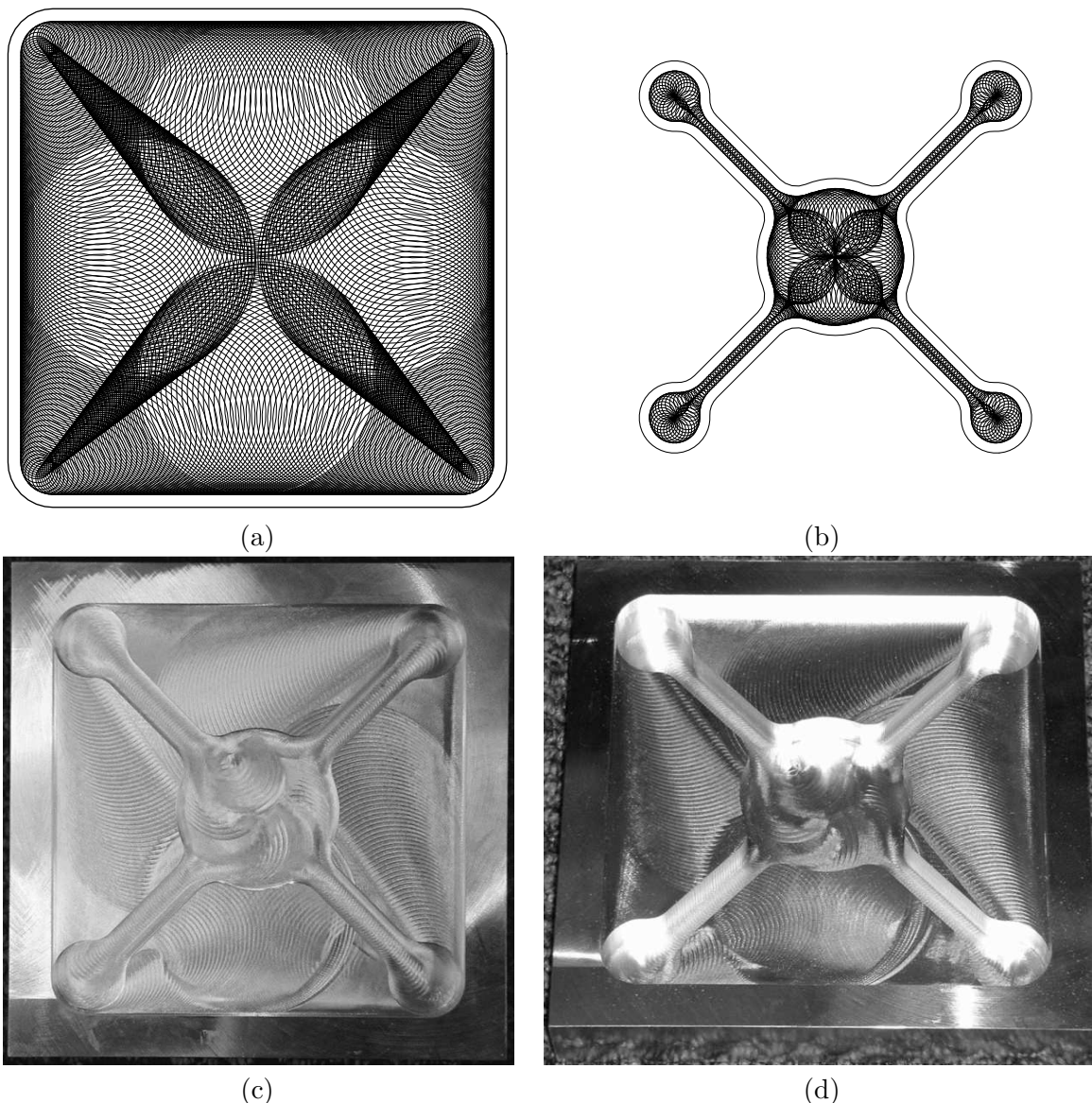


Figure 8: In (a) and (b), two stages of a one-sided MATHSM toolpath of a mold with two levels and two different pockets are presented. In (c) and (d), two views of the end part machined in aluminum are shown.

circular arc is fitted to the two successive MICs that better approximates the curvature of the outline in that neighborhood. Needless to say, such bi-tangent arcs can be made to fit in all cases where the outline is either convex, linear, or concave, achieving a better approximation of the outline and hence a superior finish for the side walls of the pocket.

Once again, let $C_i = (c_i^x, c_i^y)$ and r_i be the center point and radius of MIC \mathcal{M}_i . Assume the outline region between \mathcal{M}_i and \mathcal{M}_{i-1} is convex (as in Figure 9 and denote by κ the average curvature of the outline pocket curve between \mathcal{M}_i and \mathcal{M}_{i-1} . Then, the circular arc, \mathcal{A} , of radius $1/\kappa$ that is bi-tangent to both \mathcal{M}_i and \mathcal{M}_{i-1} will better approximate the outline, locally. The center of \mathcal{A} , $C_{\mathcal{A}} = (C_{\mathcal{A}}^x, C_{\mathcal{A}}^y)$, can be

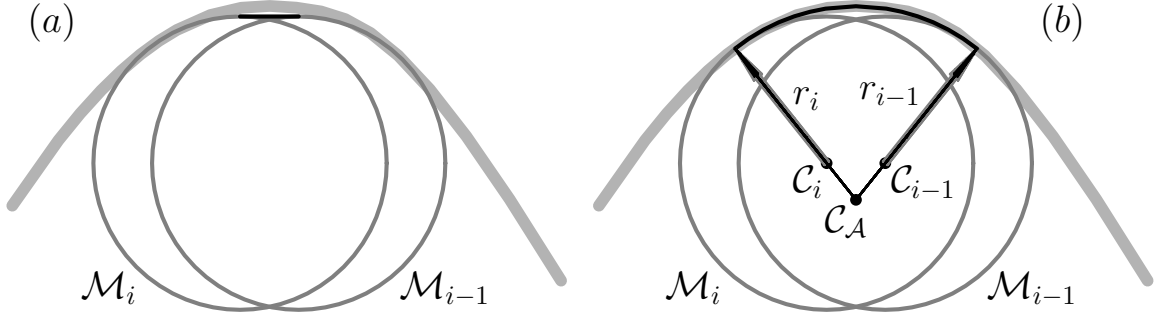


Figure 9: Two successive MICs (in dark gray) along the outline (in light gray). The linear segment (in black) that connects the two MICs in (a) is clearly inferior to the circular arc (in black) connecting the two MICs in (b). The circular arc in (b) is clearly a superior approximation for the outline, taking into consideration the second order curvature properties of the outline.

derived as,

$$\begin{aligned} \|\mathcal{C}_A - \mathcal{C}_i\| &= 1/\kappa - r_i, \\ \|\mathcal{C}_A - \mathcal{C}_{i-1}\| &= 1/\kappa - r_{i-1}, \end{aligned} \tag{3}$$

, or \mathcal{C}_A can be computed as the intersection points of two circles centered at \mathcal{C}_i and \mathcal{C}_{i-1} and of radii $1/\kappa - r_i$ and $1/\kappa - r_{i-1}$, respectively. For a concave circular arc \mathcal{A} , Equation (3) becomes

$$\begin{aligned} \|\mathcal{C}_A - \mathcal{C}_i\| &= 1/\kappa + r_i, \\ \|\mathcal{C}_A - \mathcal{C}_{i-1}\| &= 1/\kappa + r_{i-1}. \end{aligned}$$

By selecting κ_{min} instead of κ in a convex region, where κ_{min} is the minimal curvature of the outline between \mathcal{M}_i and \mathcal{M}_i , one can ensure that the fitted arc \mathcal{A} is always inside the pocket, and therefore, there is no danger of gouging. Similar arguments can be made for the containment in concave regions.

Pockets with non-planar bottoms could also benefit from the proposed scheme. Instead of a regular arc or circular motion, one should support a helical motion and adjust the height or the helical pitch based on the elevation change at the bottom of the pocket. Until now, a single MIC would have been traversed using a single G-code or NC machining command, provided the NC machine supported the circular motion of 360 degrees in a single command. With our scheme, the helical motions will have to follow the elevation of the bottom of the pocket and hence it is expected that a single circle will be broken into numerous arc segments, at the cost of a significant increase in size of the generated toolpath. The vertical slopes of the non-planar bottom geometry should also be analyzed, making sure the tool is not attempting to remove too much (too little) material at its current feed rate.

We have already mentioned that when using either the central or the one-sided MATHSM toolpath, the tool is removing material approximately half of the time. One could somewhat alleviate this fifty percent deficiency by bringing the tool more quickly to the next cutting position. Traversing \mathcal{M}_i , this goal could be achieved by either increasing the feed rate while the tool is completely contained in \mathcal{M}_{i-1} , or by shortening the length of the path while completely inside \mathcal{M}_{i-1} , at the cost of higher curvature arcs introduced into the toolpath.

When the one-sided MATHSM toolpath is used for pockets with islands, the MAT is no longer a tree and hence retractions are required. Since the toolpaths of the different loops meet along shared MAT boundaries, one can employ heuristics that connect different loops into a larger toolpath, positioning the starting (and end) point(s) of one loop at the seam with another loop, hence reducing the number of retractions. Clearly not all retractions can be removed using such a heuristic, but this number, bounded from above by the number of islands in the pocket, can be made even smaller in practice. Figure 10 again shows the hand pocket, this time with three interior islands. The MAT can no longer be traversed using a toolpath of a single loop. Yet, the two presented loops, the outer loop and the loop around island 1, can clearly be merged into one toolpath as can the two loops around islands 2 and 3. (They are not shown.)

When the radius of the MIC is changing rapidly, a redundant front can be formed in the toolpath. This effect can be seen, for example, near the bases of the five fingers, in Figures 3 and 4. The reason for this behavior can be found in the large change of radius in the MIC as the MAT and the toolpath traverse the palm into one of the fingers. In order for the toolpath to enter the finger, its MICs' radii must be significantly reduced. The radius of the MICs is decreased almost as fast as the centers of the MICs are moving forward, creating a front that is almost standing still. Equally critical is the fact that the material removal rate at the neighborhood of this front is minimal. One can clearly alleviate this toolpath redundancy by purging MICs that remove little or no material, near the front. By computing the amount of material being removed between two successive MICs (see Figure 2 (c)), one can purge away intermediate MICs that contribute below a certain threshold. Alternatively and based on the changes in the radii of the MICs, one can modify the forward steps between two successive MICs to ensure a constant amount of material removal or constant tool load.

5 Conclusion and Future Work

In this paper, we have introduced a new scheme for toolpath generation of pockets, with typically freeform outlines, toward high speed machining. The generated toolpath is C^1 continuous. Further, the central MATHSM toolpath optimizes the radial acceleration exerted on the machining tool, whereas the one-side

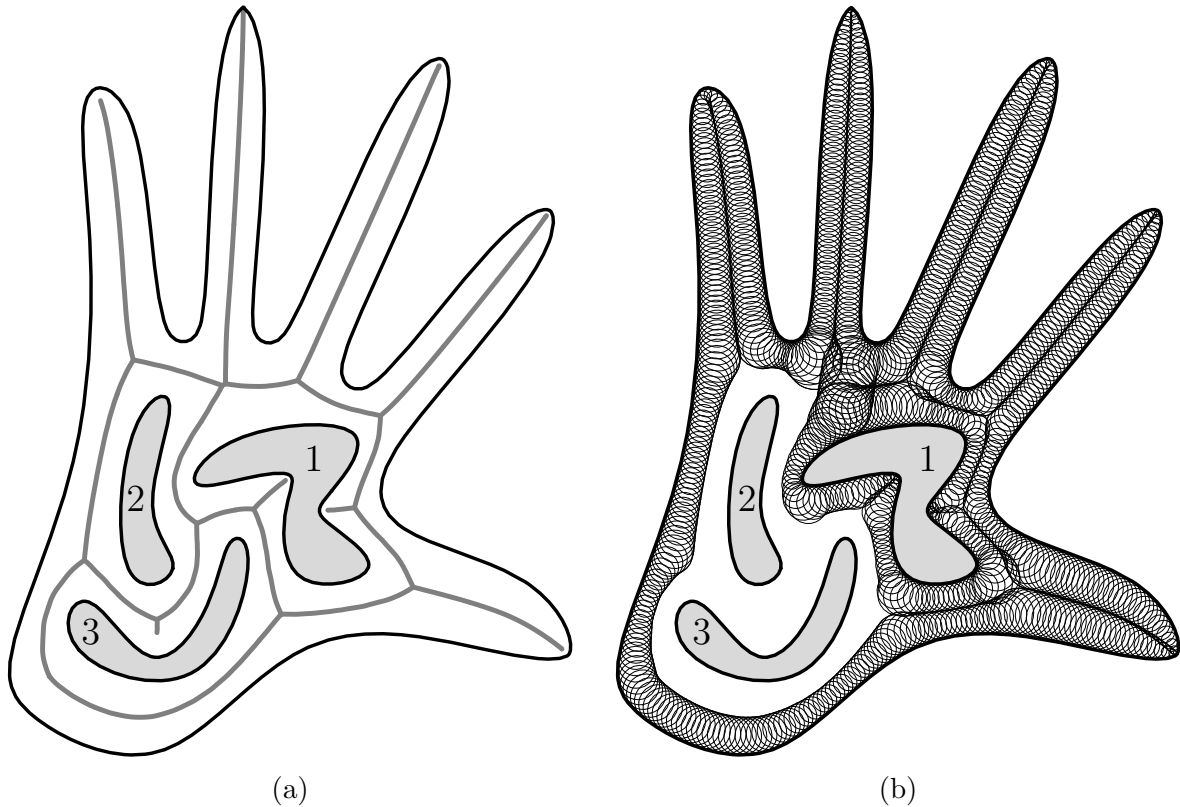


Figure 10: In (a), the MAT of a pocket with (three) islands is presented. The MAT can no longer be traversed using a single toolpath loop and cannot be completely traversed, in general, using a single path. In (b), the toolpaths for the outer loop and the loop around island 1 are shown. Clearly, these two toolpath loops could be merged into one pass without retractions as can the loops around islands 2 and 3 (not shown).

MATHSM toolpath minimizes the number of retractions—two features that are of extreme importance in high speed machining.

The MATHSM toolpath is inefficient in large rounded pocket regions, such as the palm region of the hand (Figure 6 (a)) or the rounded square shape of the mechanical mold’s pocket (Figure 8 (a)).

One can attempt more global optimization schemes and detect cases where \mathcal{M}_i cuts nothing, not due to \mathcal{M}_{i-1} , but because of previous machining operations, from different branches of the MAT of the shape. Nevertheless, even with such feasible yet complex optimization, we expect that the toolpath scheme presented in this work augment more standard approaches in regions that are long and narrow, regions where the MATHSM performs very well and more standard approaches lead to C^1 discontinuities, changes in accelerations, and multiple retractions. We foresee a global analysis scheme that will examine the geometry of a given pocket and optimize and split the work between different toolpath generation techniques, using

the MATHSM scheme in long and narrow pocket regions and traditional schemes in almost circular pocket regions.

6 Acknowledgment

The research was supported in part by ARO(DAAD19-01-1-0013) and the Fund for Promotion of Research at the Technion, Haifa, Israel. All opinions, findings, conclusions or recommendations expressed in this document are those of the author and do not necessarily reflect the views of the sponsoring agencies.

References

- [1] Y. J. Ahn, H. O. Kim and K. Y. Lee. “ G^1 arc spline approximation of quadratic Bézier curves.” *Computer Aided Design*, Vol 30, No 8, pp 615-620, 1998.
- [2] B. K. Choi and B. H. Kim. “Die-cavity pocketing via cutting simulation.” *Computer Aided Design*, Vol 29, No 12, pp 837-846, 1997.
- [3] J. J. Chou. “NC Milling Machine Toolpath Generation for Regions Bounded by Free Form Curves and Surfaces.” PhD thesis, Department of Computer Science, University of Utah, April 1989.
- [4] G. Elber, I. K. Lee, and M. S. Kim. “Comparing Offset Curve Approximation Methods.” *CG&A*, Vol 17, No 3, pp 62-71, May-June 1997.
- [5] G. Elber. “Trimming Local and Global Self-intersections in Offset Curves using Distance Maps.” The proceedings of the tenth IMA Conference on the Mathematics of Surfaces, pp ??-??, University of Leeds UK, September 2003.
- [6] R. T. Farouki and R. Ramamurthy. “Voronoi Diagram and Medial Axis Algorithm for Planar Domain with Curves Boundaries I.” *Theoretical Foundations Journal of Computational and Applied Algorithms*, 102, pp 119-141, 1999.
- [7] R. T. Farouki and R. Ramamurthy. “Voronoi Diagram and Medial Axis Algorithm for Planar Domain with Curves Boundaries II.” *Theoretical Foundations Journal of Computational and Applied Algorithms*, 102, pp 253-277, 1999.
- [8] J. D. Foley, A. van Dam, S. K. Feiner, and J. F. Hughes. “Fundamentals of Interactive Computer Graphics.” Addison-Wesley Publishing Company, second edition, 1990.

- [9] A. Hansen and F. Arbab. "An Algorithm for Generating NC Tool Paths for Arbitrarily Shaped Pockets with Islands." *ACM Transactions on Graphics*, Vol 11, No 2, pp 152-182, April 1992.
- [10] M. Held", "A Geometry-Based Investigation of the Tool Path Generation for Zigzag Pocket Machining." *The Visual Computer*, Vol 7, No 5-6, pp 296-308. September 1991.
- [11] M. Held. "Pocket Machining Based on Contour-Parallel Tool Paths Generated by Means of Proximity Maps." *Computer Aided Design*. Vol 26, No 3, pp 189-203. 1994.
- [12] M. Held. "Computing Voronoi Diagrams of Line Segments Reliably and Efficiently." *The 12 Canadian Conference on Computational Geometry*, pp 115-118, Fredericton, New Brunswick, Canada, August 2000.
- [13] E. Lee. "Contour Offset Approach to Spiral Toolpath Generation with Constant Scallop Height." *Computer Aided Design*. Vol 35, No 6, pp 511-518. 2003.
- [14] C. J. Ong, Y. S. Wong, H. T. Loh and X. G. Hong. "An optimization approach for biarc curve-fitting of B-spline curves." *Computer Aided Design*, Vol 28, No 12, pp 951-959, 1996.
- [15] H. Persson. "NC machining of arbitrary shaped pockets." *Computer Aided Design*. Vol 10, No 3, pp 169-174. 1978.
- [16] M. Ramanathan and B. Gurumoorthy. "Constructing Medial Axis Transform of Planar Domains with Curved Boundaries." *Computer Aided Design*, Vol 21, No 6, pp 371-378, July/August 2003.
- [17] Spiral high speed machining, Cimatron, <http://www.cimatron.com>.
- [18] K. Tang and S. Y. Chou and L. L. Chen. "An Algorithm for Reducing Tool Retractions in Zigzag Pocket Machining." *Computer Aided Design*, Vol 30, No 2, pp 123-129, 1998.
- [19] K. Tang and A. Joneja. "Traversing the machining Graph of a Pocket." *Computer Aided Design*, Vol 35, No 11, pp 1023-1040, 2003.
- [20] Trochoidal high speed machining, Delcam, <http://www.delcam.com>, <http://www.mmsonline.com>.
- [21] D. Veeramani and Y. S. Gau. "Selection of an Optimal Set of Cutting-Tool Sizes for 2 1/2 D Pocket Machining." *Computer Aided Design*, Vol 29, No 12, pp 869-877, 1997.